THE FIRST FULL-SCALE ACCELERATED PAVEMENT TEST IN LOUISIANA: DEVELOPMENT AND FINDINGS

by

J.B. Metcalf, S. A. Romanoschi, Y. Li, M. Rasoulian

1999

(4381 words)

J.B. Metcalf, PhD - Freeport-McMoRan Professor, Dept. Of Civil Engineering, 3502 CEBA. Louisiana State University, Baton Rouge, 70803, LA. Ph: (504) 388-4911, Fax: (504) 388-4945, e-mail: johnbm@eng.lsu.edu

S. A. Romanoschi, MSc- Graduate Research Assistant, Dept. Of Civil Engineering, 3502 CEBA, Louisiana State University, Baton Rouge, 70803, LA. Ph: (504) 388-8650, Fax: (504) 388-4945, e-mail: sromano@unix1.sncc.lsu.edu

Y. Li MSc- Graduate Research Assistant, Dept. Of Civil Engineering, 3502 CEBA Bldg, Louisiana State University, Baton Rouge, 70803, LA. Ph: (504) 388-8650, Fax: (504) 388-4945, e-mail: liyong@unix1.sncc.lsu.edu

M. Rasoulian, P.E. - Project Manager, Louisiana Transportation Research Center, 4101Gourier Av, Baton Rouge, 70808, LA. Ph: (504) 767-9112 Fax: (504) 767-9108

Metcalf J.B., Romanoschi S.A., Li Y., Rasoulian M.

ABSTRACT
The Pavement Research Facility in Port Allen, Louisiana houses the first full-scale accelerated pavement testing experiment in the state. The purpose of the first experiment was to evaluate the historically prevalent flexible crushed stone and in-place soil cement stabilized base construction in comparison to several alternative base construction materials and construction processes for pavements designed for a semi-tropical climate. Loading is provided by an Accelerated Loading Facility (ALF) machine, the second of its type in the United States. More than six million equivalent axle loads (ESALs) were applied to the nine test lanes. Performance of the pavement structures and materials was evaluated using the information provided by the monitoring of pavement surface deterioration, deflection testing during loading and post-mortem investigations. This paper presents development of the project as well as the major findings of this first experiment. The implementation of these findings in pavement design and construction practice is discussed.

Key words: full scale accelerated test, rutting, cracking, survival analysis, probability distributions

INTRODUCTION

The Louisiana Department of Transportation and Development (LaDOTD) initiated its first full scale accelerated testing program in 1992. For this program, the Louisiana Transportation Research Center (LTRC) Pavement Research Facility (PRF) was built in Port Allen, across the Mississippi river from Baton Rouge (*1*).

The Australian designed Accelerated Loading Facility (ALF) was selected as the loading device. The ALF is a transportable linear full-scale accelerated facility that imposes a rolling wheel load on a 12 m test length. Loading is unidirectional, at a constant speed of 17 km/h, distributed transversely over a 1.2m wide area. A dual tire wheel, which can be adjusted from a load of 43 to 85kN load passes every ten seconds. This allows the daily application of up to 8,100 passes (11,200 to 160,000 ESALs assuming a standard axle of 80kN and the 4^{th} power law) (*2*).

The objective of the first experiment was Ato evaluate alternative soil-cement base courses with reduced shrinkage cracking but no loss of structural capacity, by comparing the performance of nine base courses under accelerated loading to failure@.

In-place, cement stabilized select soils are the primary base material / construction technique for the vast majority of non-interstate pavements constructed in Louisiana. Such pavements typically are surfaced with 90 mm asphalt concrete. Cement stabilized soils offer a base course which is economical and easily constructed, yet provides adequate structural characteristics in an area with no crushed stone resources and high water tables. The primary factors that detract from the performance of this base type are non-uniform cement distribution, inadequate mixing of the cement and soil, and the high probability of shrinkage cracking. The non-uniformity of mixing and construction causes non-uniform support to the pavement. This results in isolated pavement failures and marked variability of the pavement performance. Cracking of the cement- stabilized bases generally results in block cracks at the pavement surface. This allows moisture to infiltrate the pavement structure and has been documented to be detrimental to rideability and performance.

TEST PROGRAM

The scope of the first experiment of the Pavement Research Facility included nine pavement lanes (Figure 1) built on a selected (A4) silty soil embankment. The 1.5m embankment was built to raise the pavements above the level of minor flooding. In order to compare the performance of the base layers, all nine lanes had the same 90mm asphalt concrete surface layer, placed in two lifts. The nine test pavements are typical of the two types used in Louisiana: flexible pavement, with a crushed limestone base (dense grading, 25mm maximum size), and semi-rigid pavement, with a soil cement base. Lane 2 with crushed stone base and lane 8 with soil-cement were the ›benchmark= pavements. The construction of the test sections followed the specifications and practices of the LaDOTD.

Three groups of three lanes were tested in sequence to ensure they were tested under similar environmental conditions.

The design of experiment allowed several direct performance comparisons:

1. lanes 2 and 8 - ›benchmark= crushed stone versus the ›benchmark= soil-cement base
2. lane 2 and 3 - 216 mm crushed stone base versus 140 mm crushed stone base with a geogrid at the base-subbase interface

3. lanes 2 and 4 - conventional crushed stone subbase versus stone-stabilized soil subbase
4. lanes 5 and 8 - in-plant versus in-place mixing of the soil-cement base
5. lanes 5 and 6 - 10 % versus 4% cement content in the in-plant mixed soil-cement
6. lanes 6 and 7 - soil-cement, 4% cement content, without and with plastic fibers (2% by weight)
7. lanes 6 and 10 - 216mm versus 305mm soil-cement base thickness, both with 4% cement
8. lanes 8 and 9 - in-place mixed soil-cement base versus an inverted crushed-stone base/cement stabilized subbase

The test lanes are instrumented with a total of 240 strain gauges and pressure cells, installed at various depths in the pavement structure. The temperatures at various depths in the asphalt layer were recorded by a weather station, also measuring air temperature, wind speed and precipitation. The watertable level was monitored using wells. Specifications, instrumentation, the data acquisition system, information on materials and the construction procedures were described by King (*1*). Since the PRF is located only one mile from the Mississipi, river stage data were obtained from the Waterways Experiment Station as an indicator of variation in water table level.

The pavement surface profile was determined using the ALF profilograph. A profile data set consists of eight transverse profiles; at 1.2 m intervals longitudinally, and three longitudinal profiles; on the centerline and at 0.3 m to the left and right. All measurements were taken at 25mm intervals.

The maximum depth under a 1.2 m straight edge was defined as the rut depth. The central longitudinal profile only is used for the determination of the surface roughness. The Slope Variance (SV) and the International Roughness Index (IRI) are computed following the procedure described by Shahin (*3*). The Slope Variance values are used to calculate the serviceability levels that allow comparison of the performance of the nine structures.

Surface cracking was recorded in relation to a coordinate grid (1.8 by 2.4 m) with cross wires at 300 mm intervals. The cracks were drawn by hand on graph paper and the length of each crack was determined. Only cracks wider than 1 mm were recorded.

Pavement surface deflections were measured by Falling Weight Deflectometer (FWD) on the centerline of the loading path of each pavement test section, at 11 stations disposed at intervals of 1.5 m along the centerline. The primary objective of FWD deflection tests on the ALF test sections was to study the change in dynamic deflection and back calculated moduli of the pavement materials, as loading progressed.

The ALF loading was applied on a single set of dual wheels (i.e. half an axle). The tire pressure was 0.724 MPa. In a cycle of 10 seconds, the wheel is in contact with the pavement for about 3 seconds, and travels 12m over the pavement surface. To simulate the real traffic the transverse loading pass distribution followed a normal distribution (*4*). The ALF wheel assembly contains a group of four-load cells that allows the measurement of the vertical load applied to the pavement structure when the wheel travels over the pavement. The system does not allow measurement of horizontal forces. During testing, the load cells indicated that the vertical load applied to the pavement is not uniform. The effect of the highest load peak, measured when the wheel touches the pavement was greatly reduced by placing a metal plate at the landing location. Even with this improvement, the vertical load is not uniform but the variability is within acceptable limits (5).

The pavements were loaded in sequence to ensure the pavements were tested under similar environmental conditions. After one lane was trafficked with 25,000 load passes the ALF machine was moved to the next lane for the same loading. During the break necessary for the move and the maintenance of the ALF machine, surface rutting and cracking, FWD and Dynaflect deflections were measured. Before starting each cycle of 25,000 ALF passes, several passes of the ALF wheel along the centerline of the lane were performed. During this, the stresses and strains at various depths in the pavement structure and the vertical ALF wheel load were measured.

Loading was terminated according to failure criteria for cracking, rutting and modulus deterioration. A rut depth of 25 mm at the surface was selected as an initial failure criterion . For cracking, a crack density of 5 m/m^2 was also regarded as failure when the cracks were distributed over more than 50 percent of the loaded area. A secondary criterion was to be any significant change in estimated pavement layer moduli (*4*). Loading was also terminated when it was judged that, in LaDOTD practice, the pavement would be rehabilitated.

In most of the cases, due to the uneven deterioration of the lanes, loading was continued beyond nominal failure in order to better observe the failure modes. This made it possible to record rut-depth values greater than 25-30mm for some transverse profiles. Table 1 records the observed failure lives.

PAVEMENT FAILURE

The primary pavement performance indicators are average rut depth and surface cracking. Their development with the number of ESALs, as well as the change in serviceability level, is reported elsewhere (5). The evolution of cracking, rutting, and serviceability level revealed that the best performing structure is the inverted pavement (lane 9) followed by the ›benchmark= crushed-stone base structure (lane2).

The response of lane 2 to loading was typical of a flexible pavement; deflection, deformation, roughness and cracking all increased with the number of passes, and at an increasing rate when the wheel load was increased.

The crack deterioration rate of lane 3 was greater than that of lanes 2 and 4 during the first period of loading. Much higher FWD deflections were also observed on lane 3 than on lanes 2 and 4 during loading, because a higher watertable existed when lane 3 was loaded. The premature failure of lane 3 is attributed mainly to this worse water condition. The premature, localized failure, with the development of a large U-shaped crack at the most heavily loaded section of the lane was unexpected. In opening the pavement it was seen that water was present at the interface between the asphalt wearing and binder courses, which could be easily separated. It was not possible to reach any conclusion on the effect of the geogrid reinforced base layer.

Lane 4 performed, and failed, in a very similar manner to lane 2, but with a shorter life. Cracking developed more rapidly than in lane 2, but rut development was slower; even though the average air temperature during testing of lane 4 (25 ^{0}C) was higher than that during testing of lane 2 (19 ^{0}C).

Lanes 5, 6 and 7 failed in a similar manner and after almost the same number of load repetitions. Extensive cracks formed before the rut depth reached the failure limit. Pumping of material through the cracks in the asphalt layer indicated erosion of material and loss of support under the asphalt surface layer.

Lane 8 failed prematurely, in an atypical manner. The typical failure for structures with stiff cement stabilized bases is due to the propagation of shrinkage cracks. Lane 8 failed due to the presence of water between the asphalt surface layer and the base course. The water caused softening and erosion of the soil cement and insufficient support was provided to the surface layer. Pumping was observed through the major cracks before the failure started. Due to the unusual, very localized failure, lane 8 was retested at a different location. This repeat test (lane 8B), failed also with formation of cracks in the asphalt layer and pumping of soil-cement through the cracks. Lane 8B had a similar life to lane 8 but the failure was not so localized.

Lane 9, the inverted pavement structure, behaved very well, and was the longest lasting pavement tested. The failure was typical for a pavement with a crushed stone base, in that the rutting was primarily due to permanent deformation in the stone layer. Fatigue cracking initiated when the stone base did not provide enough support to the asphalt layer. Thus, inverted pavements are a good solution for high moisture environments and for use over a weak subgrades. The results confirm previous theoretical and the experimental results (*6*).

Lane 10 also failed sooner than expected. The failure mechanism was similar to lane 8; the distresses were pronounced but localized.

Postmortem excavation performed after loading showed that most of the pavement rutting developed from the unbound crushed stone base layer for lane 2, 3, 4 and 9. The measurement of asphalt layer thickness, from cross section trenches and cores taken from the trafficked areas, indicated only a slight reduction of asphalt concrete layer thickness. More information on the failure mechanisms is provided by Romanoschi (*7*) and Li (*8*).

After loading ceased, more than 20 asphalt cores were taken from both the cracked and uncracked areas of crushed-stone base pavements. For all the cores, the cracks initiated at the asphalt layer surface and extended down less than 12 mm from the surface. On asphalt cores taken from the soil-cement base lanes, cracks at both the surface and the bottom of the asphalt layer were observed. Many of the cracks at the bottom of the asphalt layers were found above existing cracks in the soil-cement (*8*).

The presence of the soft soil-cement layer just below the asphalt surface layer led to the rapid failure of the soil-cement base structures. The influence of the modulus of the soft layer on the life of lane 5 was studied by Li (*8*). The analysis indicated that a change in the elastic modulus from 700KPa to 70KPa leads to an increase in the strain at the bottom of the asphalt layer by 1.3 times and to a decrease in pavement life by 2.2 times.

OBSERVED AND PREDICTED PERFORMANCE OF THE PAVEMENTS

The construction process resulted in some variability in layer thickness and material properties. The coefficient of variation of the thickness of the asphalt layer was between 2.4% and 10.4%, for example. Coupled with variability in traffic and environmental conditions this results in a nonuniform failure of the pavement; some sections of the road exhibit more severe deterioration than others.

If the difference in material characteristics, construction processes or loading levels cannot be determined, the performance of the pavement structure must be assessed by considering the information provided by both the more and less damaged zones. This way, modeling pavement deterioration will include statistical parameters that indicate the probability of attaining a certain deterioration levels under specified traffic volumes and environmental conditions.

The variability of the material stiffness is well described by the surface deflections and the backcalculated moduli. The FWD surface deflections measured the same day on all the lanes indicated a coefficient of variation for the central deflection for a lane between 3.9% and 9.4%, but a difference in central deflection of 50 percent between two adjacent stations (at 1.5 m apart) was recorded in several situations.

The stiffness of the pavement materials at the end of the construction of the nine lanes was determined by backcalculation from the FWD surface deflections (*9*). The coefficient of variation of the subgrade modulus for one lane was between 2.6% and 6.3%, but, over the entire site, subgrade moduli range between 35.9 and 91.1 MPa. The subgrade moduli value at a particular station varied significantly during the testing of the lanes due to high variation in water table level, making it difficult to estimate the strains in the pavement structure.

The backcalculated asphalt moduli were not always in the expected range (*9*). In many cases the estimated asphalt moduli values were higher than 6.89 GPa (1,000,000 psi). The coefficient of variation of the backcalculated asphalt moduli for one lane ranged between 14% and 57%. This high variation occurs because, for pavements with a thin asphalt layer, the backcalculated moduli are sensitive to the change in surface layer thicknesses. The average value of the indirect tensile modulus of the asphalt concrete at 20EC, measured on cores, was 3.0 GPa (433,000 psi), with a coefficient of variation of 22%. Similar differences between laboratory and backcalculated moduli were indicated in the literature.

The performance and material properties data collected in the experiment also allowed a comparison between the observed life of the tested pavement structures and the life predicted by mechanistic models, based on fatigue modeling of the asphalt concrete. Two life prediction models: Jameson=s model (*10*) and the Asphalt Institute model were analyzed (*11*). The first model was based on the results of the Australian ALF tests on full-depth asphalt pavements. The Asphalt Institute model was based on laboratory fatigue test results on small beams, calibrated against AASHTO data. It has a similar form to Jameson=s model, except it considers the effect of binder content and air voids on the fatigue life.

Table 1 presents the computed fatigue lives of the tested structures for the two fatigue models, along with the observed lives, for lanes 5 to 10. Since all cracks in lanes 2 to 4 were found to initiate at the surface of the asphalt layer, a comparison between the observed and fatigue predicted lives for these lanes is not possible as the theory assumes a tension crack initiating at the bottom of the layer.

The pavement failure criteria upon which Jameson=s fatigue relationship was based is defined as 50% of the trafficked area with 5.0 m/m^2 cracking. This severity and extent of cracking correspond reasonably closely to the definition of failure adopted by the Asphalt Institute, in which the fatigue relationship is for more than 45% of the trafficked area with Class 2 cracking. Due to the difference in failure criteria for fatigue cracking, the reported fatigue lives for the Jameson=s and Asphalt Institute models are different.

The results in Table 1 show that both fatigue models underpredicted the lives of lanes 6, 7 and 9 and overpredicted the life of lane 8. The observed life of lane 5 was longer than that predicted by Jamson=s model but shorter than that predicted by the Asphalt Institute method.

In order to account for the uneven deterioration of the lanes, a method based on statistical survival analysis was developed for assessing pavement life (*5*). The method consists of four steps:

A. *Establishment of the Experimental Units and Measuring Their Time-to-failure.* The tested lane is divided into panels. For each panel the time-to failure is determined after previously setting the failure criteria. After loading, some of the panels fail, others do not. The panels that do not fail are censored observations.

B. *Derivation of Non-Parametric Time-to-failure models*. The time-to-failure is modeled using a discrete probability distribution function that has constant values in the intervals between two consecutive failures. The probability distribution model is derived using the Kaplan-Meier algorithm, which takes into consideration the failure observations as well as the censored observations.

C. *Derivation of Parametric Time-to-failure Models.* The time-to-failure is modeled using a ›classical= continuous probability distribution function. The parameters of the continuous distribution are computed based on the maximum-likelihood principles. The distribution selected for modeling the time-to-failure must have a simple form and an increasing hazard function. The hazard function at a time ›t= is the probability that a panel will fail in the next time unit knowing that it had not failed before the time ›t=, and therefore it needs to increase continuously.

D. *Comparison of the Derived Time-to-failure Models with Other Pavement Life Models*. The lognormal distribution was used to derive the median observed pavement life since it has a simple form, an increasing hazard function and allows the comparison with the life predicted by the AASHTO structural design method for flexible pavements (*12*). The AASHTO design equation assumes that the life of the pavement structure follows a lognormal distribution. When two distributions are lognormal, a modified student t-test can be used to investigate how close the observed life distribution is to the design life distribution.

The ALF lanes were divided into eight panels, 1.25m long and 1.8m wide each. The failure criteria was 25mm for the rut depth or $5m/m^2$ over 50% of the loaded area for the cracking extent. On each panel, one transverse profile and crack density were recorded at every 25,000 passes of the ALF machine. All the lanes were loaded even after some panels failed to determine the life of other panels. Only when the deteriorations were very severe was loading stopped. The pothole developed on lane 10 was patched with cold asphalt mix and the loading continued another 25,000 ALF passes until the patching failed. Since only two panels failed when lanes 3 and 8 were tested initially, these lanes were retested to increase the number of failed panels.

The results of the pavement life probability models are also reported in Table 2. The AASHTO design lives were estimated using typical layer coefficients and the designed layer thicknesses, a subgrade modulus of 30MPa (4,350psi) and a standard deviation of 0.35. The results indicate that, the lives of lanes 2 and 9 were longer than the corresponding predicted lives; the life of lane 4 was slightly shorter but close to the design life, while the lives of all the other lanes were shorter than the predicted lives. Justifications for the reduced life of several pavements are given by the failure mechanisms.

An interesting case is that of lane 3 where the pavement structure performed much better for the second test than in the first test, mainly due to large differences in the water table levels. The statistical survival analysis model for the time-to-failure reflects the premature failure of the structure in the first test. The statistical method does not explain how the moisture condition in the foundation layers affected the performance of lane 3 and the retested lane 3B.

PERFORMANCE OF THE MATERIALS AND STRUCTURES - DIRECT COMPARISON

The design of the experiment allowed direct comparison of the performance of materials and structures leading to the following conclusions:

1. The ›benchmark‹ crushed-stone base structure (lane 2) outperformed the ›benchmark‹ soil-cement structure (lane 8). All stabilized base structures failed due to softening and erosion of the materials and loss of support under the asphalt layer. Shrinkage cracks in the stabilized base generated reflection cracks in the asphalt surface layer.
2. It was not possible to assess the effect of the geogrid placed at the base/subbase interface of lane 3, due to premature failure, possibly due to effects of the moisture condition in the foundation layers;
3. No significant difference was found between the performance of in-place or in-plant mixed soil-cement bases, since lanes 5 and 8 had similar performances and failure modes;
4. The higher cement content (10%) in the in-plant mixed soil-cement (lane 5) only slightly increased the life of the structure when compared to the low-cement content (4%) of the stabilized base (lane 6);
5. The plastic fibers (lane 7) do not increase significantly the performance of the soil-cement base (lanes 7 and 6).
6. At the same cement content, increasing the thickness of the soil-cement (lane 10 vs. lane 6) improves the performance of the road structure.
7. Under high moisture conditions, an inverted pavement (lane9) outperforms the soil-cement base pavement (lane 8), as well as the conventional flexible pavement (lane 2).

CONCLUSIONS

A. The Louisiana ALF experiment has been successfully conducted and appropriate loading and data processing methods established.

B. The performance of two ›benchmark‹ pavements (lanes 2 and 8) has been documented for this and future experiments.

C. The survival model and two fatigue models gave reasonable predictions of pavement life. However, the AASHTO design for cement stabilized bases over predicted life under ALF loading.

D. Consideration can be given to the implementation of four practical findings;

-the use of an AASHTO layer coefficient of 0.10 for stone stabilized base
-the use of the inverted pavement configuration
-the use of thicker cement stabilized bases with lower cement contents
-the lack of evidence of any advantage in pavement life from the use of fibre reinforcement in cement stabilized layers or from the placement of a geogrid in an unbound base.

Confirmation of these findings by an in-service road trial is desirable to evaluate longer term effects and to assess costing and construction issues.

E. Consideration should be given to inclusion of more sophisticated moisture movement detection technology in future ALF experiments.

REFERENCES

1. King, W.M., Gillespie K. and G. Crosby. *Construction and Comparison of Louisiana=s Conventional and Alternative Base Courses under Accelerated Loading*, LTRC Report 93-1ALF, Louisiana Transportation Research Center, Baton Rouge, 1997.

2. Metcalf J.B., *The Application of Full Scale Accelerated Pavement Testing*. NCHRP Synthesis 235, Transportation Research Board, National Research Council, Washington, DC., 1997.

3. Shahin M.V. *Pavement Management for Airports, Roads, and Parking Lots*. Chapman & Hall: New York, 1994.

4. Li Y., Metcalf J.B., Romanoschi S.A. and M. Rasoulian, Development of the Louisiana ALF Program: the First Experiment, Paper presented at the 1998 TRB Annual Meeting, Transportation Research Board, Washington, D.C., 1998.

5. Romanoschi S.A., Metcalf J.B., Li Y. and M. Rasoulian. Results From The First Full-scale Accelerated Pavement Test Project in Louisiana. Paper presented at the 1999, TRB Annual Meeting, Transportation Research Board, Washington, D.C., 1999. (In press)

6. Tutumluer E. and R.D. Barksdale. Inverted Flexible Pavement Response and Performance. In *Transportation Research Record 1482*, TRB, National Research Council, Washington, D.C., 1995.

7. Romanoschi S.A., Metcalf J.B., Li Y. and M. Rasoulian. Assessment of Pavement Life at the First Full-scale Accelerated Pavement Test in Louisiana. Paper presented at the 1998 TRB Annual Meeting, Transportation Research Board, Washington, D.C., 1998.

8. Li Y., Metcalf J.B., Romanoschi S.A. and M. Rasoulian, Soil-Cement Base Pavements under Accelerated Loading, Paper presented at the 1999 TRB Annual Meeting, Transportation Research Board, Washington, D.C., 1999. (In press)

9. Romanoschi S.A. *The Correlation between the Structural Number and the Falling Weight Deflections for Louisiana roads*. Master=s Thesis, Louisiana State University, Baton Rouge, 1996.

10. Jameson G.W., K.G. Sharp, and N.J. Vertessy. *Full-depth asphalt pavement fatigue under accelerated loading: The Mulgrave (Victoria) ALF trial*, 1989/1991. Australian Road Research Board, 1992.

11. Shook, J. E., F. N. Finn, M. N., Witczak, and C. L., Monismith. Thickness design of asphalt pavements: The Asphalt Institute Method. *Proceedings of the 5th International Conference on the Structural Design of Asphalt Pavements*, Ann Arbor, Vol.1, pp. 17-44, 1982.
12. A.A.S.H.T.O., *AASHTO Guide for Design Of Pavement Structures*, American Association of State Highway and Transportation Officials, Washington, D.C., 1993.

TABLE 1. Design, Predicted and Observed Life (ESALs x 1,000)

Lane	Jameson=s Model		Asphalt Institute		Survival Analysis Observed	AASHTO Design
	Observed	Predicted	Observed	Predicted		
2	-	-	-	-	600	484
3	-	-	-	-	174*	233
4	-	-	-	-	347	373
5	207	150	170	232	289	1038
6	210	93	180	171	254	1038
7	233	114	189	145	265	1038
8	310	3336	234	1536	308	826
9	1250	241	1220	276	1170	1095
10	-	8160	-	2754	532	844

*first failure only

FIGURE 1. The Configuration of the PRF Test Lanes B thickness in mm

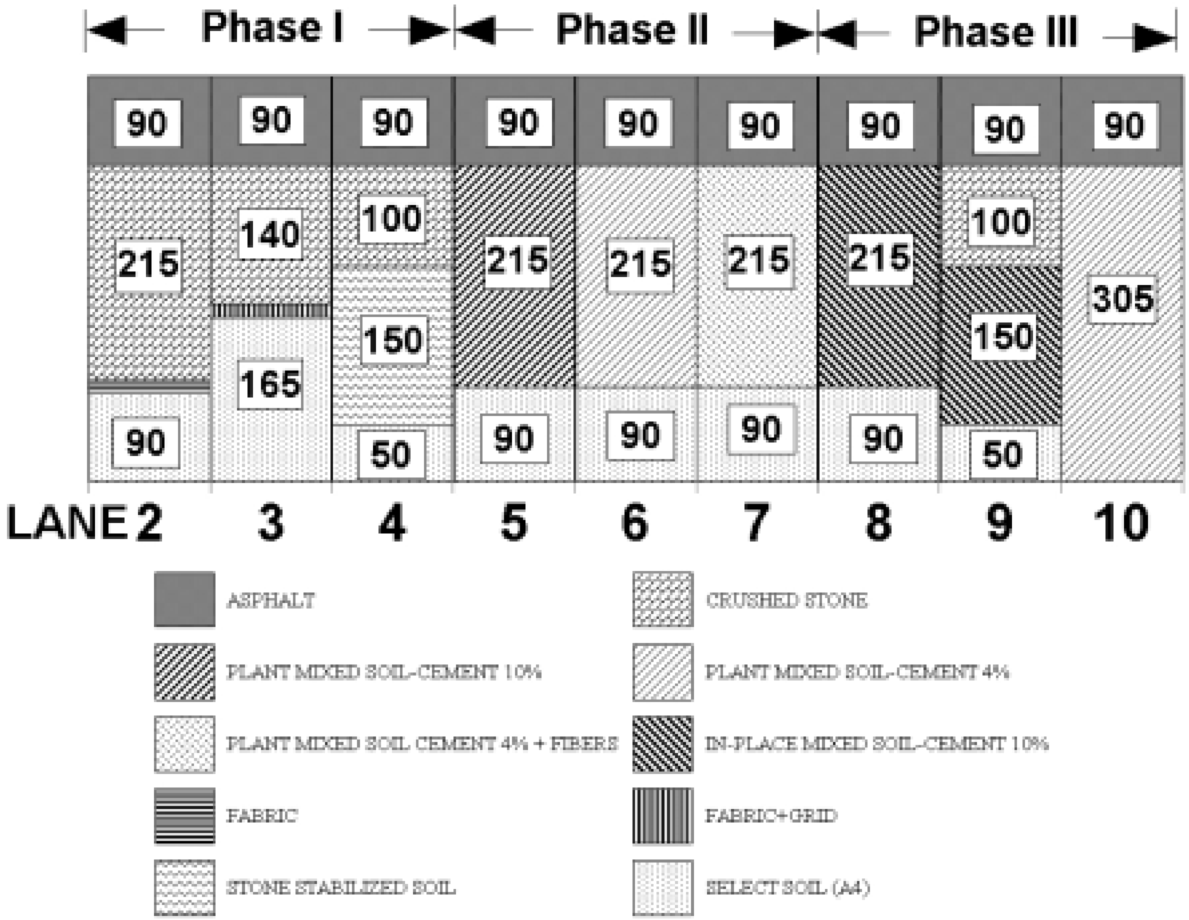

Slide 1

Louisiana Transportation Research Center, which is a joint effort of LSU (BR) and the LaDOTD has initiated its first full-scale accelerated pavement testing program in 1992. For this program, the Pavement Research Facility (PRF) was built in Port Allen, LA, across the Mississippi River from Baton Rouge.
The Australian designed ALF machine was selected as loading device.
I will discuss today the development of the first three experiments

Slide 2

The first experiment started in February 1996 , the objective of the experiment being …………….. To fulfill the objective, nine pavement structures, having the same AC surface layer were constructed. Three groups of three lanes have been loaded in sequence to ensure they are tested under similar environmental conditions.

Slide 3

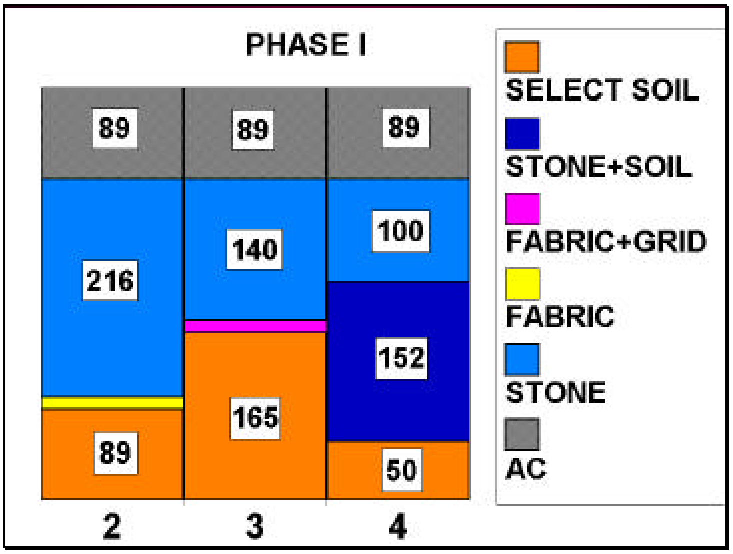

Lanes tested in phase I of the project (Lanes 2,3 and 4) have crushed stone bases. A geogrid was placed at the subbase - subgrade interface of lane 3.

Here we have a direct comparison aimed to determine the performance of a thinner aggregate base reinforced with a geogrid (lane 3) or with a stone stabilized soil subbase (lane 4), lane 2 being the reference-benchmark pavement structure

These lanes were tested between January and October 1996

Slide 4

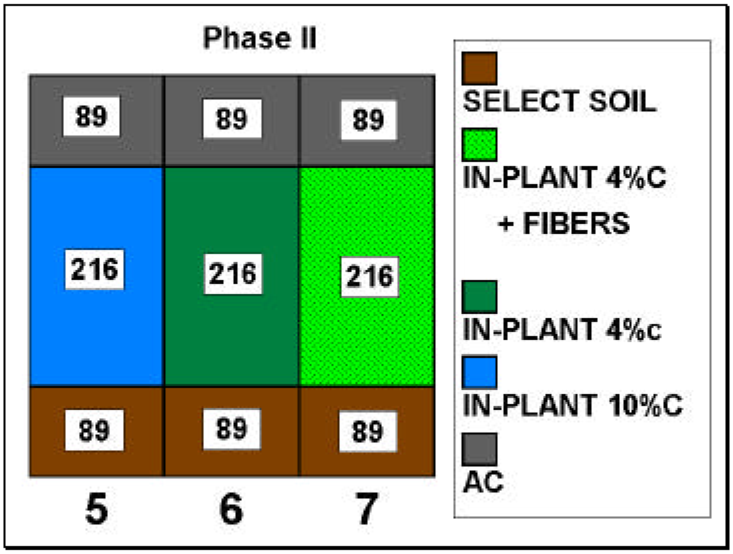

Lanes tested in the phase II of the project have soil-cement bases, with the same thickness but different cement contents, or soil-cement with fibers (lane7)

Here, the direct comparison aims to determine if the reduction in cement content (from 10% to 4%) decreases significantly the performance of the base layer, and if the plastic fibers improve significantly the performance of the soil-cement base.

Here lane 5 is the benchmark structure and represents the current practice in Louisiana.

Slide 5

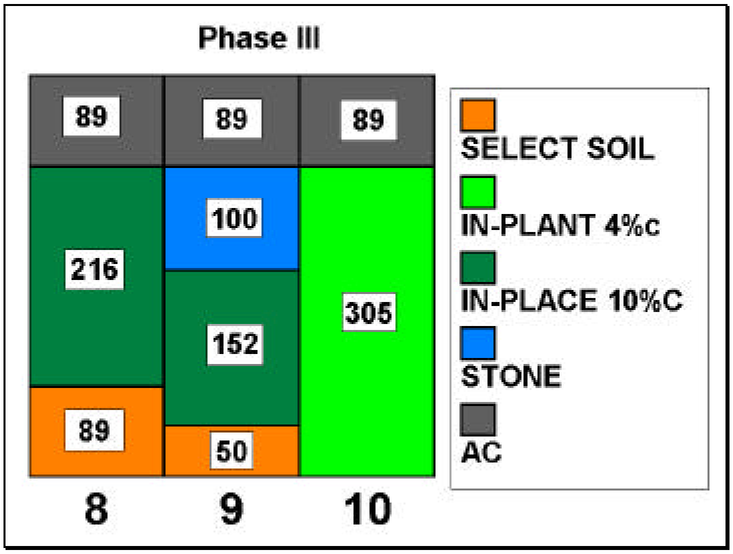

Lanes tested during phase III have a cement treated base (8 and 10) or subbase (9). Lane 9 is an inverted pavement structure with a crushed stone base and a in-place mixed cement stabilized soil.
This phase aims to determine if a thicker but softer soil-cement layer performs better than a thin but stronger (10%) soil-cement base. It also allowed to compare the effectiveness of in-place (lane 8) vs. the in-plant mixing (lane5).
Lane 9 is an inverted pavement and helped us determine if an aggregate base interlayer can significantly increase pavement life.
The construction of the test sections followed the specification and practices recommended by LaDOTD

Slide 6

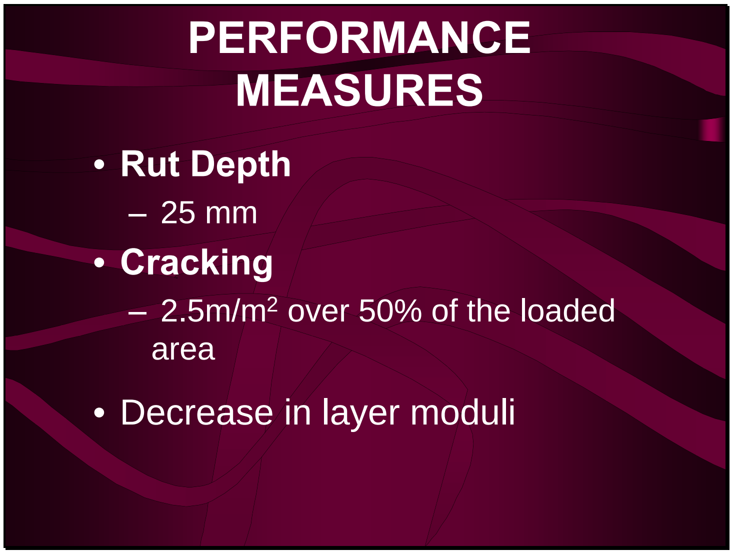

The condition of the pavement structure was continuously monitored during testing. The pavement surface longitudinal and transverse profiles, FWD and Dynaflect surface deflections, stress and strains at various depths in the structure were measured about every 25,000 passes.
An increase in rut depth of 25 mm at the surface (average for the 8 transversal profiles), and a crack density of 5 m/m2 over 50% of the loaded area were selected as primary failure criteria.
A secondary criteria was the decrease in base and surface layer moduli.

Slide 7

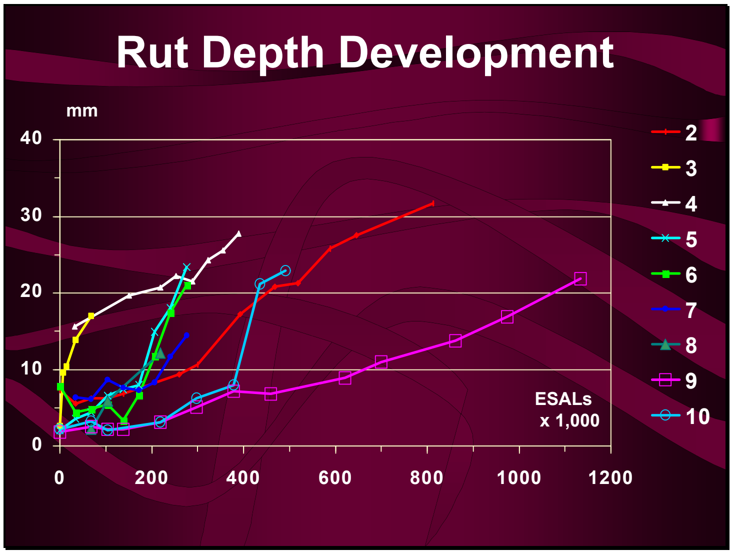

The first indicator of pavement condition is the average rut depth, determined from 8 transverse profiles. This figure presents its development with loading (expressed in Equivalent Standard Axle Loads).
It can be noticed that the rut depth did not reach 20 mm for lanes 3 and 8 (YELLOW and GREEN) since they failed due to severe localized cracking. The best performing from point of view of the rut depth evolution is lane 9 (MAGENTA), the inverted pavement, that reached the failure criteria after 1,200,000 ESALs.
Lanes 2 (RED) and 10 (BLUE - CIRCLE) also had a slow increase in rutting.

Slide 8

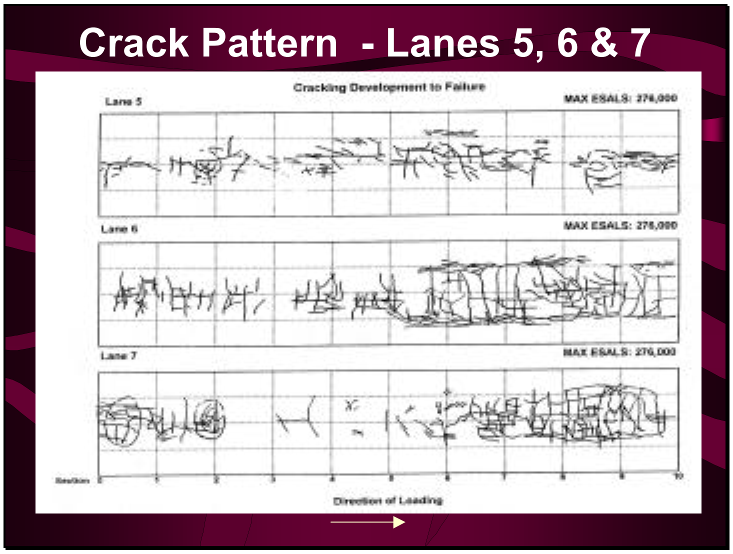

This figure presents the crack pattern at the end of loading, for lanes tested during phase II, all having soil-cement bases. The crack development is more uniform, with cracks extended over the entire tested areas.

Slide 9

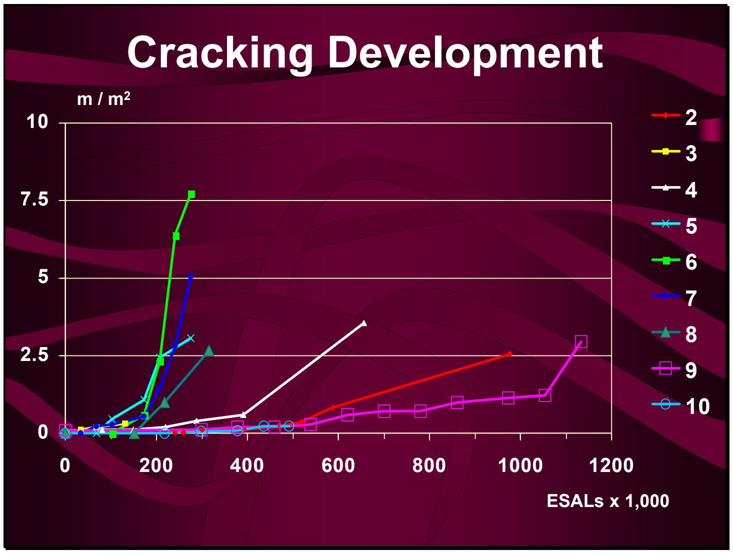

This figure presents the evolution of cracking (in m/m2). Again, we can see that cracks initiated and developed slower for lane 2, 4 and 9 - the inverted pavement, that for the other lanes.
Sudden failure occurred in lanes 3 and 8 (YELLOW and DARK GREEN), with development of large potholes in the most heavily loaded area. Testing was repeated on these lanes, re-testing of lane 3 being in progress. This is possible since the lanes are 200 feet - 60 meters long and the travel length of the ALF wheel is 12 meters.

Slide 10

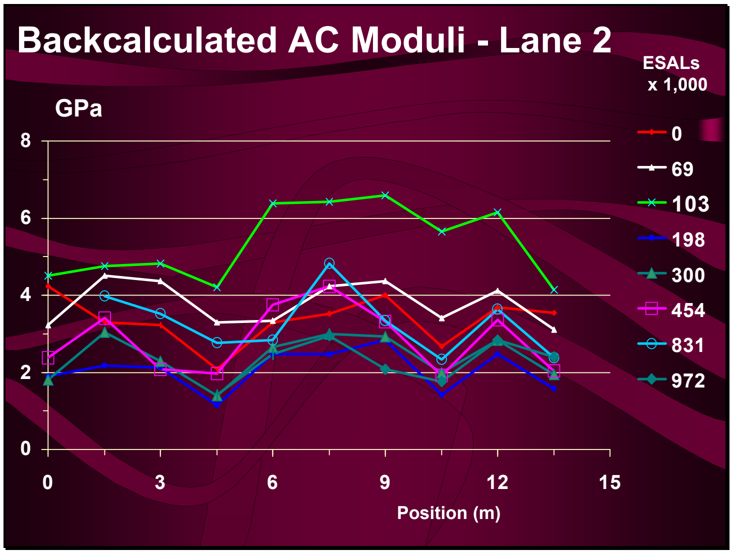

High non-uniformity of the surface deflection along the lanes were obtained for most of the lanes.

The backcalculated subgrade modulus presented high variations, mainly due to the clayey foundation and the variable water table level.
Before testing, the coefficient of variation for the backcalculated AC modulus for one lane was between 15 and 56 %, compared with 22% obtained for the moduli measured in the laboratory.
For the subgrade modulus, the coefficient of variation along one lane was between 3 and 6 %, but over the entire site, the moduli values ranged between 35 and 90 MPa.

Slide 11

This graph presents the evolution of the serviceability level with loading (ESALs). Again, we can see that the best performing pavement structure tested so far in this experiment is lane 9, the inverted pavement. It had the slowest decrease in serviceability level. Lanes 3 and 8 failed suddenly so the serviceability level at the end of their life was not computed.

Slide 12

PAVEMENT LIFE

Lane	Rutting	Cracking	PSI	Design
2	628	966	825	484
3	-	146	146	233
4	359	574	488	373
5	351	235	269	1038
6	449	198	296	1038
7	725	231	305	1038
8	-	304	304	824
9	1207	1138	1348	1095
10	654	496	496	844

This table presents the pavement life in thousand of ESALs for:
the rutting life - when the rutting limit of 25mm was reached (in some cases the life was computed by extrapolation)
the cracking life (5m/m2) over 50 of the loaded area
the serviceability - life to a terminal serviceability level of 2.5
Also, we compared these values with the design values, computed using the LADOTD procedure based on the SN concept. The reliability level selected was 50%.
From this table we can see that the lives of lanes 2, 4 and 9 was longer than expected, while the life of all other lanes was shorter than expected.
Lanes 3 and 8 failed prematurely, lane 3 due to the loss of bond between the two asphalt lifts, lane 8 due to rapid erosion of the soil-cement material just below the asphalt layer. This led to the loss of support under the asphalt surface layer and the rapid failure of the structure.

Slide 13

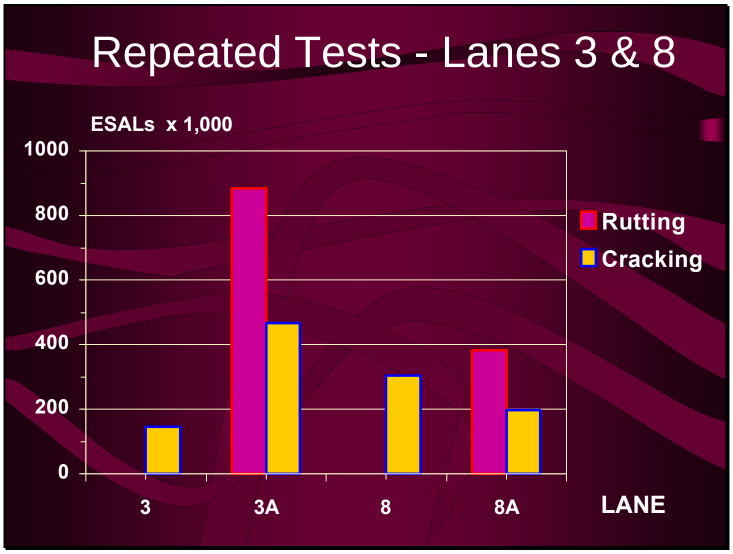

Considering that lanes 3 and 8 failed abnormally, we have retested these lanes in different locations (the lanes were 60 m long and the testing area is only 12 m long.

For lane 8, we observed the same type of failure in both tests, with extensive cracking, distributed over the entire loading area. The cracking lives were similar.

When we retested lane 3, (Fall 98) the water table was much lower than in the first test, and therefore the cracking and rutting lives were much higher. Considering the great effect of the water table level, it is very difficult to evaluate the performance of lane 3, and thus, that of the geogrid reinforcement.

We believe that replicate tests are useful, in many instances they may eliminate doubts in terms of premature failures and failure modes.

Slide 14

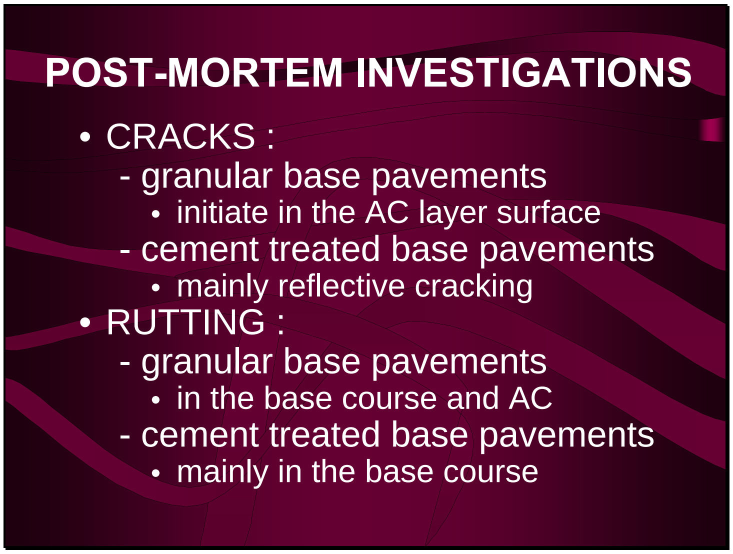

The post-mortem investigation provided useful information on the mechanisms of crack and rut depth development.

After loading was stopped, more than 20 asphalt cores were taken from the granular base lanes, from both cracked and un-cracked areas. The fatigue cracks developed from the asphalt concrete surface and extended less than 12.5mm deep from the surface. Not a single crack was found on the bottom of the cores from both cracked and un-craked areas.

For the soil-cement base structures, extensive cracks were found in the cement stabilized material when the AC layer was removed.

The most severe cracks reflected through the AC surface layer.

Cracks also initiated at the bottom of the AC layer but did not always reached the pavement surface.

Transverse profiles measured at the post-mortem trenches revealed that rutting is mainly developed in the base course, in both granular and soil-cement bases.

Slide 15

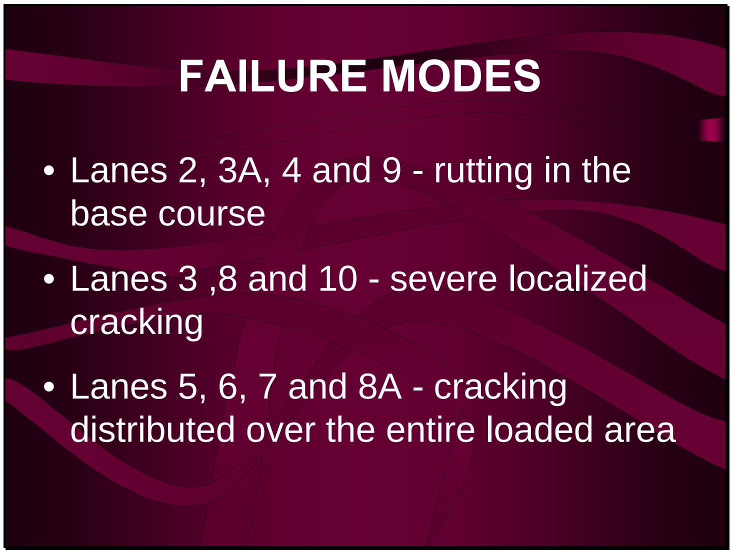

From the degradations observed at pavement surface, as well as from the post-mortem evaluations, it was concluded that lanes 2, 4 and 9 failed primarily due to rutting in the crushed stone base course.
Lanes 3, 8, and 10 failed prematurely, lane 3 due to the loss of bonding and presence of water between the two asphalt lifts; lanes 8 and 10 the due to erosion of the soil-cement base just below the asphalt layer.
Lanes 5, 6, and 8A (repeated test on lane 8), failed due to cracking in the asphalt layers, either reflection cracking from the soil-cement base or fatigue cracking in the asphalt due to the failure of the base.

Slide 16

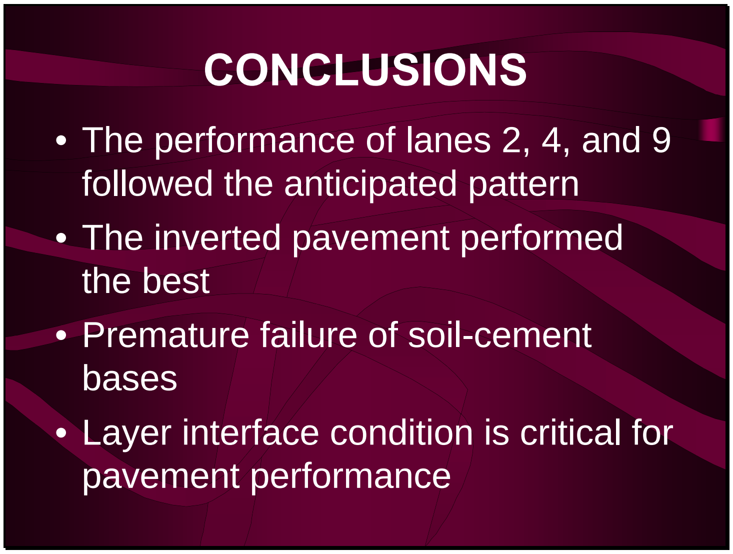

Three of the lanes, 2, 4 and 9 followed the anticipated pattern, failing by rutting in the granular base course. All other lanes had shorter lives than expected.

The inverted pavement behaved very well, it was the longest lasting pavement tested so far in this experiment, the structure being less sensitive to high moisture levels in the foundation layers. Therefore, the inverted structures are a good solution for high moisture environments and for use over weak subgrades.

Under high moisture conditions, the material at the top of the soil-cement layer softened, erodes, and does not provide support to the asphalt surface layer. From here, the poor performance of soil-cement bases in Louisisana climatic conditions.

The layer interface condition is a critical factor in pavement performance. The inadequate bonding between layers leads to redistribution of stresses and strains in the pavement structure and thus to premature failures. The presence of water at the interface accelerates the degradation process.

Slide 17

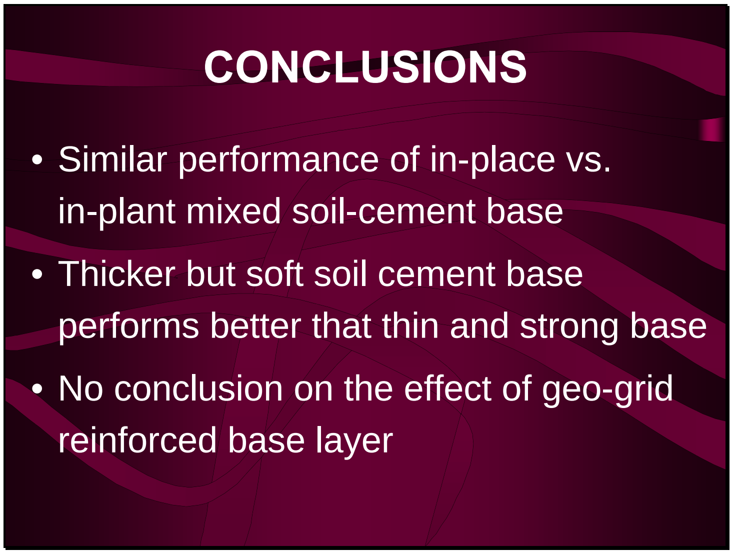

In-place mixed soil-cement base has a similar performance with the in-plant mixing.
For high moisture environments, a thicker soil-cement base layer with a low cement content performs better than a thinner layer with higher cement content.
Due to the abnormal failure of lane 3, due to the loss of bond between the two asphalt layers, no conclusion could be drawn regarding .the benefic effects of the geogrid reinforcement.

Slide 18

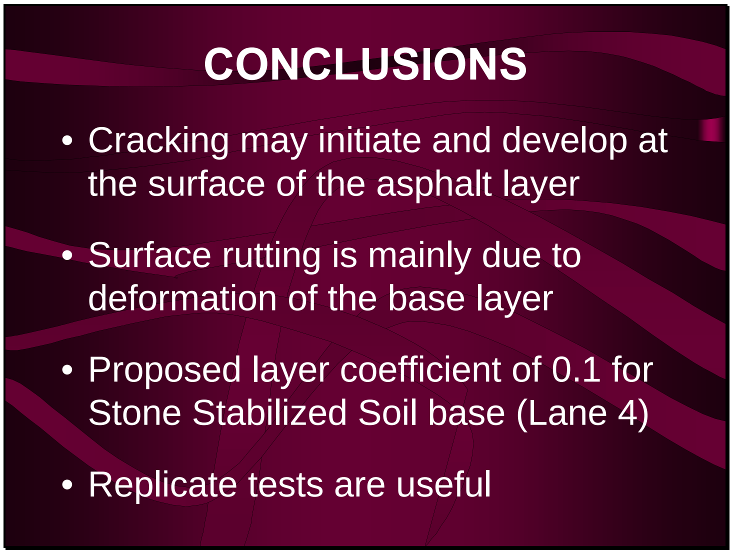

Contrary to the general assumtion that cracks initiate at the bottom of the asphalt surface layer, we found that cracks may initiate at pavement surface, probably due to high horizontal forces.

Rutting in asphalt pavement in wet environments is mainly cause by settlements into the granular or stabilized base layer

A recommended value for the structural layer coefficient for the stone-stabilized soil subbase is 0.1 but further observation of in-service pavements having this subbase is necessary to validate this value.

Replicate tests are useful even expensive. They can be used to validate experiments, in term of failure mode and structural life.

Slide 19

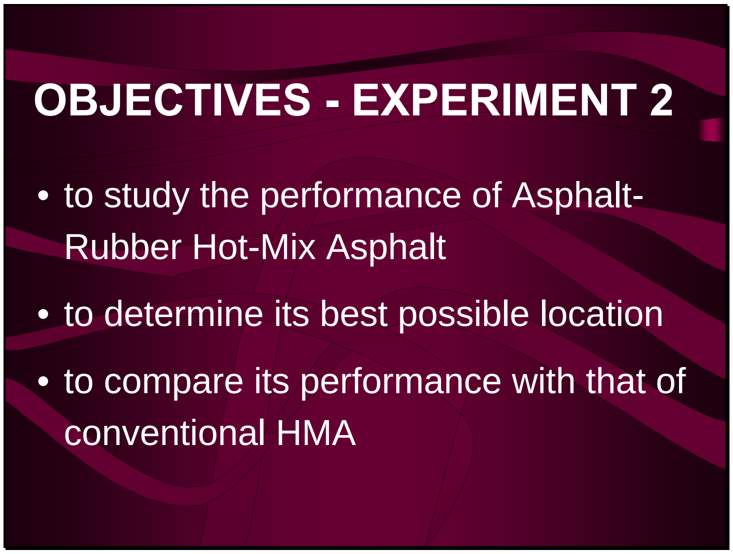

The objective of the experiment is ……………..

Slide 20

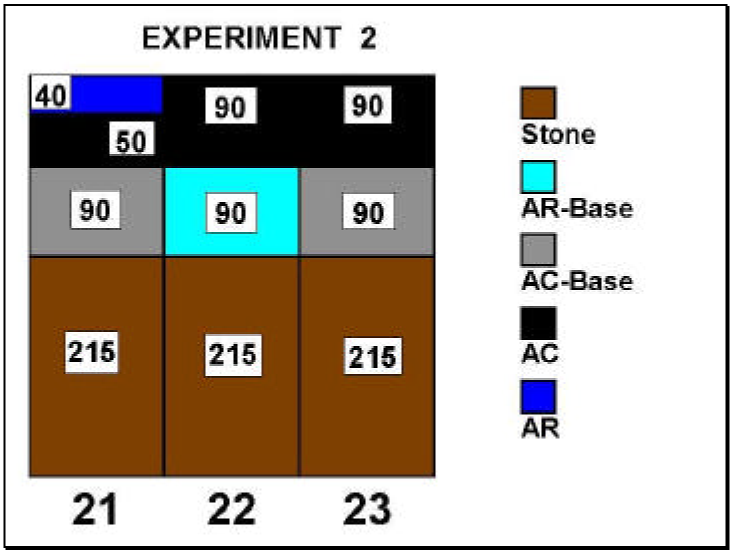

These are the three structures we are currently testing.
Lane 21 has a AR-HMA wearing course, lane 22 has an AR_HMA base layer and lane 23 is the conventional full-depth asphalt structure.
All three pavements have crushed stone subbgrades, and the embankment for these pavement was a 10% soil-cement.
We strengtened the embankment so we can assure that the failure will be in the upper layers

Slide 21

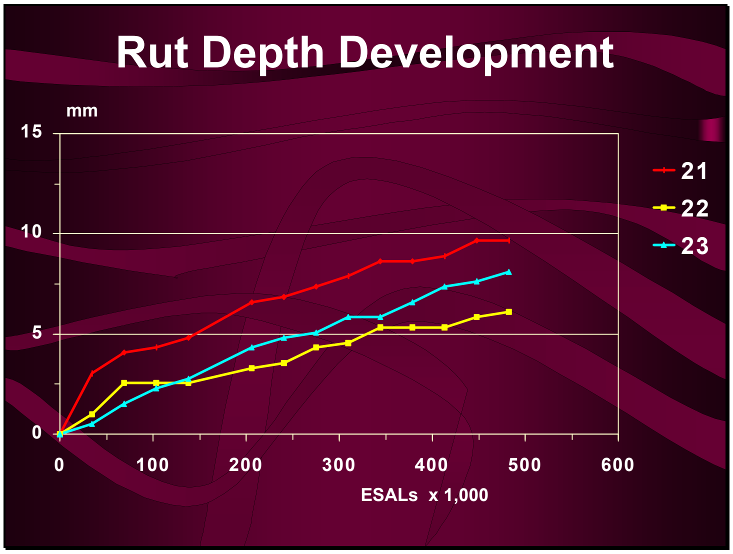

We have applied around 0.5 million ESALs to each of these structures.

A preliminary result of this test is the average rut depth, determined from 8 transverse profiles. The rut depth indicates that Asphalt Rubber material used in the wearing course may lead to higher rutting than the typical HMA, without any rubber.

Lower rut depths were recorder for lane 22, having an AR base layer.

So far we haven’t observed any cracks, we will evaluate the AR mix function of the cracking development too.

Slide 22

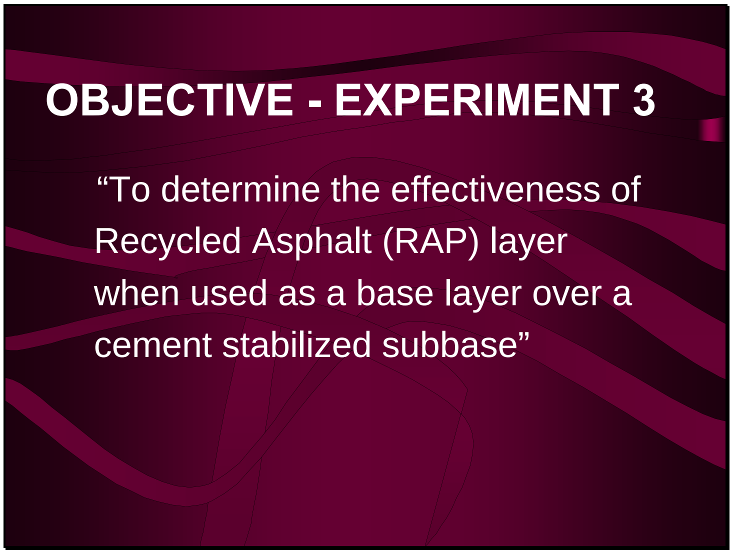

The following experiment aims to determine…. Recycled asphalt consists in milling of the distress asphalt concrete layer into pieces of   size. This may be a promising solution for the repair of many damaged semi-rigid pavements in Louisiana.
It is estimated that this material is could behave similarly if not better than the conventional inverted pavement structure with a crushed stone base.

Slide 23

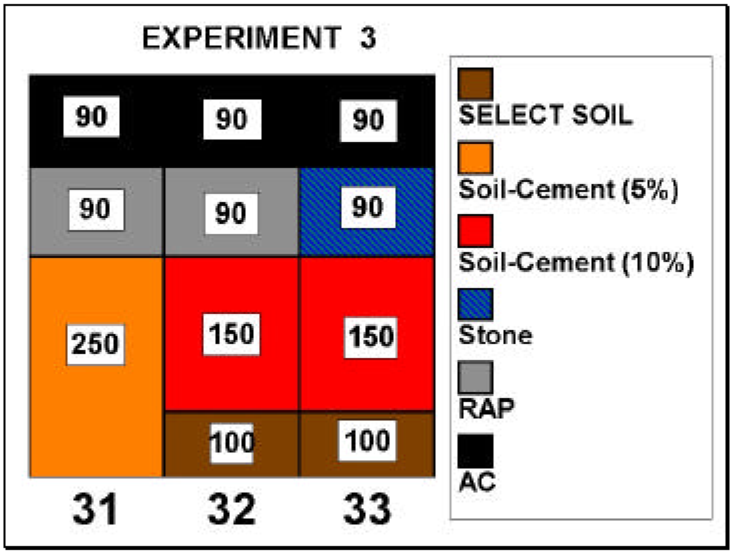

This figure presents the three test pavements:
Lane 31 with a RAP base over a soft but thick subbase,
lane 32 with a RAP base over a stiff and thinner subbase
Lane 33, the benchmark inverted pavement structure with crushed stone base over a soil-cement subbase.
These lanes are already built, we estimate that they will be tested next Spring.